Temperature-dependent phonon dynamics of supported and suspended monolayer tungsten diselenide

Cite as: AIP Advances **9**, 085316 (2019); https://doi.org/10.1063/1.5118004
Submitted: 02 July 2019 . Accepted: 11 August 2019 . Published Online: 22 August 2019

Thais C. V. Carvalho, Francisco D. V. Araujo, Clenilton Costa dos Santos, Luciana M. R. Alencar, Jenaina Ribeiro-Soares, Dattatray J. Late, Anderson Oliveira Lobo, Antonio Gomes Souza Filho, Rafael S. Alencar, and Bartolomeu C. Viana

Temperature-dependent phonon dynamics of supported and suspended monolayer tungsten diselenide

Cite as: AIP Advances 9, 085316 (2019); doi: 10.1063/1.5118004
Submitted: 2 July 2019 • Accepted: 11 August 2019 •
Published Online: 22 August 2019 • Corrected: 27 August 2019

Thais C. V. Carvalho,[1] Francisco D. V. Araujo,[2] Clenilton Costa dos Santos,[3] Luciana M. R. Alencar,[3] Jenaina Ribeiro-Soares,[4] Dattatray J. Late,[5,6] Anderson Oliveira Lobo,[7] Antonio Gomes Souza Filho,[8] Rafael S. Alencar,[9,a)] and Bartolomeu C. Viana[1,2,b)]

AFFILIATIONS

[1]Departament of Physics, Federal University of Piauí, Teresina, Piauí, 64049-550, Brazil
[2]LIMAV-Interdisciplinary Laboratory of Advanced Materials, Materials Science and Engineering Graduate Program (PPGCM), Federal University of Piauí, Teresina, Piauí, 64049-550, Brazil
[3]Department of Physics, Federal University of Maranhao, São Luíz, Maranhão, 65.085-580, Brazil
[4]Department of Physics, Federal University of Lavras, Lavras, Minas Gerais, 37200-000, Brazil
[5]Physical and Materials Chemistry Division, CSIR-National Chemical Laboratory, Dr Homi Bhabha Road, Pune 411008, India
[6]Academy of Scientific and Innovative Research (AcSIR), Ghaziabad 201002, India
[7]LIMAV-Interdisciplinary Laboratory of Advanced Materials, Materials Science and Engineering Graduate Program (PPGCM), Federal University of Piaui, Teresina, Piaui, 64049-550, Brazil
[8]Departament of Physics, Federal University of Ceará, Fortaleza, Ceará, 60455-900, Brazil
[9]College of Physics, Federal University of Pará, Belém, Pará, 66075-110, Brazil

[a)]**Electronic mail:** rsalencar@ufpa.br.
[b)]**Electronic mail:** bartolomeu@ufpi.edu.br.

ABSTRACT

Two-dimensional materials exhibit great potential for high-performance electronics applications and the knowledge of their thermal properties is extremely necessary, since they are closely related to efficient heat dissipation and electron-phonon interactions. In this study we report the temperature-dependence of the out-of-plane A_{1g} Raman mode of suspended and supported CVD-grown single-crystalline tungsten diselenide (WSe_2) monolayer. The A_{1g} phonon wavenumber is linearly red-shifted for temperature ranging from 98 to 513 K, with first-order temperature coefficients β of -0.0044 and -0.0064 cm^{-1}/K for suspended and supported monolayer WSe_2, respectively. The higher β module value for supported sample is attributed to the increase of the phonon anharmonicity due to the phonon scattering with the surface roughness of the substrate. Our analysis of the temperature-dependent phonon dynamics reveal the influence of the substrate on thermal properties of monolayer WSe_2 and provide fundamental information for developing of atomically-thin 2D materials devices.

The remarkable electronic and optical properties of two-dimensional (2D) materials, which come from the in-plane quantum confinement effect, have attracted great attention of the scientific community for exploiting these systems. These 2D materials include graphene, hexagonal boron nitride (hBN), transition metal dichalcogenides (TMDs) and phosphorene[1–4] among others. TMDs with a common composition of MX_2 (M=Mo, W, Nb, Ta, Re; X=S, Se, Te) offer a wide range of electronic properties, from superconducting to semi-metallic, and also to semiconducting behaviour.[5,6] In particular, semiconducting TMDs have received considerable attention due to their tunable energy band gaps (from 1 to 3 eV). These particular characteristics offer opportunities for the development of novel

electronic, optoelectronic, chemical and biomedical devices for which semi-metallic graphene is not suitable for.[7–9] Both WS_2 and MoS_2 have emerged as essential components of photoactive devices with various functionalities, such as field effect transistors (FETs),[10,11] photoconductors,[12–14] photovoltaics,[15,16] rewritable memories,[17] etc.

WSe_2 exhibits an electronic band structure similar to its sulfide counterpart, i.e. it experiences an indirect-to-direct band gap transition as the crystal is reduced from bulk to monolayer.[18,19] The unique band structure along with the reduced dimensionality of few-layer WSe_2 enables atomically thin systems to display numerous novel phenomena, such as pronounced photoluminescence and the manipulation of the valley degrees of freedom of charge carries.[18,20,21] The strong light-matter interactions observed in WSe_2 thin layers make them excellent candidates to be used in optoelectronic circuits.[22–24] All these remarkable electronic properties are related to the thermal characteristics and therefore an efficient heat dissipation is necessary to reach high-performance on electronic devices. Therefore, the detailed knowledge of thermal properties of few-layered TMDs is extremely relevant.[25,26]

In order to understand the vibrational properties of TMDs, it is important to correlate them with the phonon transport and the electron-phonon interactions, which can determine the performance of electronic devices, due to non-harmonic effects in the lattice potential energy. Thus, the changes promoted by the temperature variation in the band positions of Raman spectroscopy can give us information about the thermal properties of 2D materials.[27–35]

Raman spectroscopy is a widely used technique to identify the number of atomic layers and thermal properties of TMDs layers.[36–40] Previous reports have shown the dependence of Raman modes and thermal properties when the TMDs layers were suspended or supported, thus showing that the surface effect plays an important role to TMDs devices functionalities.[26,29–34,41–43] Thus, to the best of our knowledge, temperature-dependent Raman spectroscopy of suspended monolayer WSe_2 has not been investigated yet and the thermal properties study of this suspended TMD it is very important for future applications based on WSe_2.

In this work, we report a temperature-dependent study of the Raman spectra of suspended and supported monolayer WSe_2 obtained by Chemical Vapor Deposition (CVD). The changes observed in the A_{1g} mode wavenumber data with temperature were measured and the first-order temperature coefficient for supported and suspended samples were calculated within the framework of phonon decay mechanism. The differences in the phonon anharmonicity were interpreted as being due to the scattering of phonons by the surface roughness of the substrate. Our findings provide fundamental information about the phonon dynamics of monolayer WSe_2 from the extraction of temperature coefficients of the suspended and supported samples, which is useful for thermal

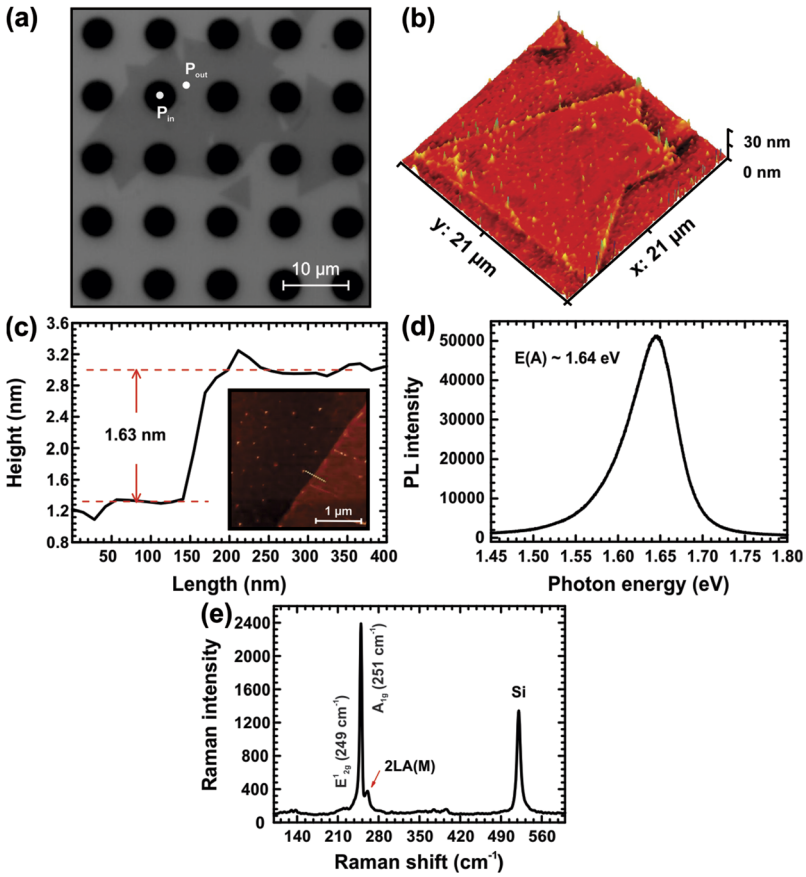

FIG. 1. (a) Optical and (b) AFM images of monolayer WSe_2. The white dotes are the position where the Raman spectra were recorded on suspended (P_{in}) and supported WSe_2 sample (P_{out}). (c) Height profile acquired along the dashed lines shown in the inset. (d) PL and (e) Raman spectra of the WSe_2 sample.

management in various optoelectronic devices and applications of WSe_2.

Suspended single-crystalline monolayer WSe_2 sample, grown through CVD on SiO_2/Si substrate, was purchased from 2DLayer company. The sample thickness was estimated by atomic force microscopy (AFM), Raman and photoluminescence (PL) spectroscopies. AFM measurements of WSe_2 samples were performed using a Multimode 8 microscope (Bruker, Santa Barbara, CA) in Quantitative Nanomechanics (QNM) mode using probes model Scanasyst Air, with nominal spring constant of 0.4 N/m and nominal tip radio of 2 nm approximately. Images resolution were of 512 samples per lines. Sample analysis was performed with NanoScope Analysis1.50 software. Figure 1 (a) shows an optical image of a selected region with suspended monolayer WSe_2 on a hole with ~ 5 μm of diameter. Topographic image recorded in tapping mode of a characteristic WSe_2 flake is shown in Figure 1 The thickness measured on the borders of the flake was found as being 1.6 nm thick (Figure 1 (c)), which correspond to two layers.[44] On the other hand, PL and Raman spectra, (Figures 1 (d) and (e), respectively) of the same flake are characteristic of monolayer WSe_2.[18,45] The overestimated height measured by AFM could be attributed to possible polymer contaminants presents on the sample surface due to the transfer process of the sample.

Raman spectroscopy experiments were performed using a Bruker Senterra spectrometer with a spectral resolution of 3 cm^{-1}. To focus the laser beam and to collect the Raman signal it was used an Olympus BX5 microscope equipped with a 50X (0.35 NA) objective lens mounted in a backscattering geometry. A solid-state laser line with 2.33 eV (532 nm) excitation energy was used for measuring the Raman spectra with the power kept below 500 μW to avoid sample overheating. Each spectrum was recorded with 10 coadditions with 10 seconds of integration time. The temperature-dependent measurements were performed in a Linkam thermal stage THMS600.

PL measurements were done through a T64000 Jobin Yvon spectrometer equipped with nitrogen cooled charge-coupled-device detector and a diode pumped solid state laser with 2.33 eV (532 nm) excitation energy. An Olympus BX41 microscope coupled with a 100X objective lens (0.9 NA) was used to focus and acquire the backscattered signal.

In the bulk form, WSe_2 crystal belongs to space group $P6_3/mmc$ and it is expected the existence of seven first-order Raman-active modes at the center of the Brillouin zone, distributed among the irreducible representations as E^2_{2g}, E_{1g}, E^1_{2g} and A_{1g} (the modes labeled with the letter "E" are doubly degenerate in the layer plane[46]).[47,48] The E^2_{2g} mode corresponds to a shear mode between

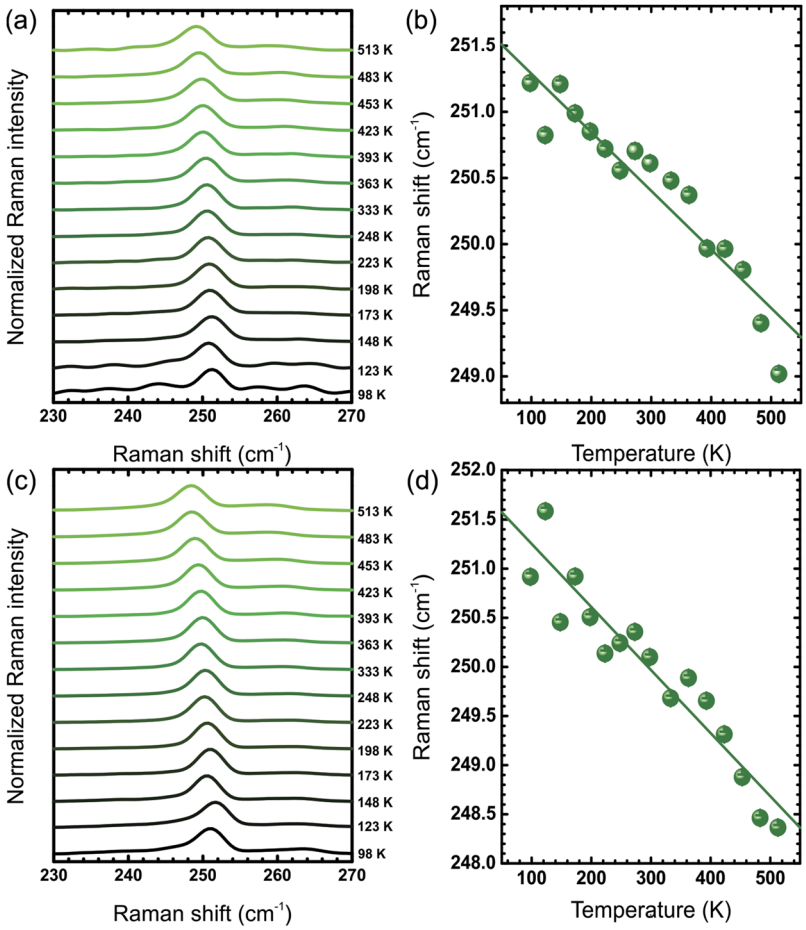

FIG. 2. Normalized Raman spectra of monolayer WSe_2 measured at different temperatures for suspended (a) and supported (c) sample, collected at P_{in} and P_{out} position indicated in Figure 1 (a), respectively. Temperature-dependence of the A_{1g} mode for (c) suspended and (d) supported monolayer WSe_2. The linear fitting parameters for experimental data in (b) and (d) panels are listed in Table I.

two rigid layers against each other. The E_{1g} mode is an in-plane vibration related to Se displacements and its observation is forbidden in a backscattering geometry perpendicular to the basal plane. The E^1_{2g} mode corresponds to a in-plane movement of Se and W atoms, whilst the A_{1g} mode involves an out-of-plane vibration of Se atoms.[45] These two modes exhibit similar frequencies and the E^1_{2g} mode is observed as a weak shoulder located at lower energy side of the A_{1g} band. The frequencies of these modes, denoted from now on as $\omega_{E^1_{2g}}$ and $\omega_{A_{1g}}$, are located at about 249 cm^{-1} and 251 cm^{-1}, respectively.[45,49] Our study is focused on the most intense A_{1g} mode for the excitation energy used.

Figure 2 (a) shows the Raman spectra of suspended monolayer WSe_2 in the of 230-270 cm^{-1} spectral range measured at temperatures varying from 98 to 513 K. For clarity all spectra were normalized regarding the maximum intensity and vertically shifted. An intense peak is observed at about 251 cm^{-1} and it is associated to the A_{1g} phonon mode. Upon increasing temperature, this phonon mode experiments a red-shift as well as an increasing in the full width at half maximum (FWHM) of the peak, in agreement with previous studies on supported monolayer and bulk WSe_2.[41,50–52] A similar result is observed for monolayer WSe_2 supported on SiO_2, as can be seen in Figure 2 (c).

For a more accurate analysis of the temperature-dependent Raman wavenumber (ω), we performed a line-shape analysis of the A_{1g} phonon mode using a Lorentzian profile for each temperature value. The temperature-dependence of ω is showed in the Figure 2 (b) and (d), for suspended and supported monolayer WSe_2.

In order to fit the temperature-dependence of the A_{1g} mode, we used a simplified anharmonic phonon decay model, based on Balkanski's approach,[53] where higher order temperature coefficients have not been taken into account, since they are not significant in the temperature range that we measured:[26,28]

$$\omega(T) = \omega_0 + \beta T, \tag{1}$$

where ω_0 is the Raman wavenumber of A_{1g} mode at absolute zero temperature (T = 0 K) and β is its first-order temperature coefficient.

The displacement of the Raman modes with the temperature at constant pressure is mainly due to thermal expansion and volume contributions. Considering that ω (Raman phonon frequency) as a function of the temperature and volume as shown below,[41,54]

$$\left(\frac{\partial ln\omega}{\partial T}\right)_P = \left(\frac{\partial lnV}{\partial T}\right)_P \left(\frac{\partial ln\omega}{\partial V}\right)_T + \left(\frac{\partial ln\omega}{\partial T}\right)_V = \frac{\gamma}{\kappa}\left(\frac{\partial ln\omega}{\partial P}\right)_T + \left(\frac{\partial ln\omega}{\partial T}\right)_V \tag{2}$$

Where, $\gamma \approx (\partial lnV/\partial T)_P$ is the volume thermal coefficient and $\kappa \approx -(\partial lnV/\partial P)_T$ is the isothermal volume compressibility. The first term from the right-hand side of the equation 2 provide the volume contribution at constant temperature and the second term express the temperature contribution at constant volume. The values of isobaric temperature and isothermal pressure from the phonon frequencies of the modes can provide the anharmonic contribution. The double resonance phenomenon is very active in single layer sample and can explain changes in the intensity and shift in the peak position as a function of temperature.[41]

Table I shows the obtained ω_0 and β for our suspended and supported monolayer WSe_2. The results obtained in supported monolayer WSe_2 and bulk WSe_2 taken from the Refs. 41, 50, 51 and 52, respectively, were listed for comparison. The Raman data for suspended monolayer WSe_2 presented the smallest β value as compared to supported monolayer and bulk WSe_2.

The Grüneisen parameter γ is an important thermoelastic value which relate the thermodynamic properties of a solid to its vibrational frequencies in a material.[52] It describes the changes of cell volume caused by temperature and pressure, and indicates the anharmonic effects on the phonon spectrum.[51] The isobaric mode Grüneisen parameter γ_{iP} is associated to temperature coefficient β by means of the equation:[52]

$$\gamma_{iP} = -\frac{1}{\alpha\omega_i}\beta_i, \tag{3}$$

where ω_i is the Raman wavenumber of the i^{th} phonon mode (in this study is $\omega_{A_{1g}}$ and it is calculated from the intercept on the $\omega_{A_{1g}}$ versus temperature plot, as shown in Figures 2 (b) and (d)) and α is the thermal expansion coefficient.

As a first approximation, we used the thermal expansion coefficient α from bulk WSe_2[52] to calculate the γ_{iP} and the results are shown in Table I. We also compared our findings with those for supported monolayer and bulk taken from the Refs. 51 and 52, respectively. Since the thermal conductivity (κ) is proportional to γ^{-2},[55] the suspended monolayer WSe_2 presents higher κ.

The scattering by optical phonons has been observed to limit electrical transport and heat dissipation.[56–58] Therefore, we attribute

TABLE I. A_{1g} mode Raman wavenumber at T = 0 K (ω_0) and first-order temperature coefficient (β) of supported and suspended monolayer and bulk WSe_2. The isobaric mode Grüneisen parameter $\gamma_{A_{1g}P}$ was calculated according to Eq. 3, by using in a first approximation the expansion coefficient alfa from bulk WSe_2.[52]

Sample	Mode	ω_0 (cm^{-1})	β (cm^{-1}/K)	$\gamma_{A_{1g}P}$	Temperature range (K)
Suspended monolayer WSe_2	A_{1g}	251	−0.0044	0.73	98-513
Supported monolayer WSe_2	A_{1g}	251	−0.0064	1.06	98-513
Supported monolayer WSe_2[51]	A_{1g}	252	−0.009	1.39	175-575
Supported monolayer WSe_2[41]	A_{1g}	248	−0.0071	–	80-539
Supported monolayer WSe_2[50]	A_{1g}	255	−0.0067	–	77-623
Bulk WSe_2[52]	A_{1g}	251	−0.0085	1.39	80-300

the higher $\gamma_{A_{1g}}$ (higher anharmonicity and lower κ) for supported WSe_2 as being due to decreasing of the phonon life-time (which is closely related to phonon coherence length) caused by the scattering with the surface roughness of the substrate, as has been recently proposed for monolayer gallium sulfide (GaS).[59]

In summary, we performed a temperature-dependent study of the Raman spectrum of suspended and supported monolayer WSe_2 in order to probe the influence of the substrate in the phonon anharmonicity and thermal properties. Our results show that the A_{1g} mode wavenumber experiments a linear downshift in 98-513 K temperature range. The first-order temperature coefficient β was estimated as being -0.0044 and -0.0064 cm^{-1}/K for suspended and supported monolayer WSe_2, respectively. The observed differences in β is explained as due to the increase of the phonon anharmonicity caused by the scattering with the surface roughness of the substrate. The results presented here are important to shed light on the influence of the substrate on the thermal conductivity of 2D systems.

BCV acknowledges the support from CNPq PVE 400397/2014-5, the Produtividade em Pesquisa-PQ-2016 305632/2016-7, Universal 427084/2018-0 and FAPEPI ENERGIAS RENOVÁVEIS 001/2018. RSA acknowledges the supports from CAPES (Grant No. 88887.162565/2018-00). AGSF acknowledges the financial support from CNPq (Grant 309309/2017-4) and CAPES (Procad 183995). CCDS acknowledges the financial support from FAPEMA (UNIVERSAL-01290/16). JR-S thanks the Foundation for Research Support of Minas Gerais (FAPEMIG Grants No. CEX-APQ-01865-17, No. TEC-AUC-00026-16, No. RED-00185-16, No. RED-00282-16), the National Council for Scientific and Technological Development (CNPq Grants No. 310813/2017-4, 433027/2018-5), the Agency for Financing Studies and Projects - FINEP (02/2014 DMOL No. 0058/16 and NANO No. 0501/16, and 02/2016), and also the support from the Pró-Reitoria de Pesquisa and Pró-Reitoria de Gestão (UFLA) and the prize L'ORÉAL-UNESCO-ABC Prêmio Para Mulheres na Ciência (For Women in Science Prize - Brazil/2017).

REFERENCES

[1] K. S. Novoselov, D. Jiang, F. Schedin, T. J. Booth, V. V. Khotkevich, S. V. Morozov, and A. K. Geim, "Two-dimensional atomic crystals," Proceedings of the National Academy of Sciences **102**, 10451–10453 (2005).
[2] M. Xu, T. Liang, M. Shi, and H. Chen, "Graphene-like two-dimensional materials," Chemical Reviews **113**, 3766–3798 (2013).
[3] H. O. H. Churchill and P. Jarillo-Herrero, "Phosphorus joins the family," Nature Nanotechnology **9**, 330–331 (2014).
[4] M. Chhowalla, Z. Lin, and M. Terrones, "Themed issue on 2d materials," J. Mater. Chem. C **5**, 11156–11157 (2017).
[5] X. Huang, Z. Zeng, and H. Zhang, "Metal dichalcogenide nanosheets: Preparation, properties and applications," Chem. Soc. Rev. **42**, 1934–1946 (2013).
[6] M. Chhowalla, H. S. Shin, G. Eda, L.-J. Li, K. P. Loh, and H. Zhang, "The chemistry of two-dimensional layered transition metal dichalcogenide nanosheets," Nature Chemistry **5**, 263–275 (2013).
[7] D. Jariwala, V. K. Sangwan, L. J. Lauhon, T. J. Marks, and M. C. Hersam, "Emerging device applications for semiconducting two-dimensional transition metal dichalcogenides," ACS Nano **8**, 1102–1120 (2014).
[8] Q. Wang, K. Kalantar-Zadeh, A. Kis, J. Coleman, and M. Strano, "Electronics and optoelectronics of two-dimensional transition metal dichalcogenides," Nature Nanotechnology **7**, 699–712 (2012).
[9] M. C. Demirel, M. Vural, and M. Terrones, "Composites of proteins and 2d nanomaterials," Advanced Functional Materials **28**, 1704990 (2018).
[10] B. Radisavljevic, A. Radenovic, J. Brivio, V. Giacometti, and A. Kis, "Single-layer MoS_2 transistors," Nature Nanotechnology **6**, 147–150 (2011).
[11] J. K. Ellis, M. J. Lucero, and G. E. Scuseria, "The indirect to direct band gap transition in multilayered MoS_2 as predicted by screened hybrid density functional theory," Applied Physics Letters **99**, 261908 (2011).
[12] N. Perea-López, Z. Lin, N. R. Pradhan, A. Iñiguez Rábago, A. L. Elías, A. McCreary, J. Lou, P. M. Ajayan, H. Terrones, L. Balicas, and M. Terrones, "CVD-grown monolayered MoS_2 as an effective photosensor operating at low-voltage," 2D Materials **1**, 011004 (2014).
[13] A. Sobhani, A. Lauchner, S. Najmaei, C. Ayala-Orozco, F. Wen, J. Lou, and N. J. Halas, "Enhancing the photocurrent and photoluminescence of single crystal monolayer MoS_2 with resonant plasmonic nanoshells," Applied Physics Letters **104**, 031112 (2014).
[14] Z. Yin, H. Li, H. Li, L. Jiang, Y. Shi, Y. Sun, G. Lu, Q. Zhang, X. Chen, and H. Zhang, "Single-layer MoS_2 phototransistors," ACS Nano **6**, 74–80 (2012).
[15] M. Fontana, T. Deppe, A. K. Boyd, M. Rinzan, A. Y. Liu, M. Paranjape, and P. Barbara, "Electron-hole transport and photovoltaic effect in gated MoS_2 Schottky junctions," Scientific Reports **3**, 1634 (2013).
[16] S. Wi, H. Kim, M. Chen, H. Nam, L. J. Guo, E. Meyhofer, and X. Liang, "Enhancement of photovoltaic response in multilayer MoS_2 induced by plasma doping," ACS Nano **8**, 5270–5281 (2014).
[17] K. Roy, M. Padmanabhan, S. Goswami, T. P. Sai, G. Ramalingam, S. Raghavan, and A. Ghosh, "Graphene- MoS_2 hybrid structures for multifunctional photoresponsive memory devices," Nature Nanotechnology **8**, 826–830 (2013).
[18] W. Zhao, Z. Ghorannevis, L. Chu, M. Toh, C. Kloc, P.-H. Tan, and G. Eda, "Evolution of electronic structure in atomically thin sheets of WS_2 and WSe_2," ACS Nano **7**, 791–797 (2013).
[19] A. Splendiani, L. Sun, Y. Zhang, T. Li, J. Kim, C.-Y. Chim, G. Galli, and F. Wang, "Emerging photoluminescence in monolayer MoS_2," Nano Letters **10**, 1271–1275 (2010).
[20] X. Xu, W. Yao, D. Xiao, and T. F. Heinz, "Spin and pseudospins in layered transition metal dichalcogenides," Nature Physics **10**, 343–350 (2014).
[21] B. Liu, M. Fathi, L. Chen, A. Abbas, Y. Ma, and C. Zhou, "Chemical vapor deposition growth of monolayer WSe_2 with tunable device characteristics and growth mechanism study," ACS Nano **9**, 6119–6127 (2015).
[22] A. Pospischil, M. M. Furchi, and T. Mueller, "Solar-energy conversion and light emission in an atomic monolayer p-n diode," Nature Nanotechnology **9**, 257–261 (2014).
[23] J. S. Ross, P. Klement, A. M. Jones, N. J. Ghimire, J. Yan, D. G. Mandrus, T. Taniguchi, K. Watanabe, K. Kitamura, W. Yao, D. H. Cobden, and X. Xu, "Electrically tunable excitonic light-emitting diodes based on monolayer WSe_2 p-n junctions," Nature Nanotechnology **9**, 268–272 (2014).
[24] B. W. H. Baugher, H. O. H. Churchill, Y. Yang, and P. Jarillo-Herrero, "Optoelectronic devices based on electrically tunable p-n diodes in a monolayer dichalcogenide," Nature Nanotechnology **9**, 262–267 (2014).
[25] B. Peng, H. Zhang, H. Shao, Y. Xu, X. Zhang, and H. Zhu, "Thermal conductivity of monolayer MoS_2, $MoSe_2$ and WS_2: Interplay of mass effect, interatomic bonding and anharmonicity," RSC Adv. **6**, 5767–5773 (2016).
[26] A. G. Vieira, C. Luz-Lima, G. S. Pinheiro, Z. Lin, J. A. Rodríguez-Manzo, N. Perea-López, A. L. Elías, M. Drndić, M. Terrones, H. Terrones, and B. C. Viana, "Temperature- and power-dependent phonon properties of suspended continuous WS_2 monolayer films," Vibrational Spectroscopy **86**, 270–276 (2016).
[27] A. A. Balandin, "Phonon engineering in graphene and van der Waals materials," MRS Bulletin **39**, 817–823 (2014).
[28] A. A. Balandin, S. Ghosh, W. Bao, I. Calizo, D. Teweldebrhan, F. Miao, and C. N. Lau, "Superior thermal conductivity of single-layer graphene," Nano Letters **8**, 902–907 (2008).
[29] Thripuranthaka M and D. J. Late, "Temperature dependent phonon shifts in single-layer WS_2," ACS Applied Materials & Interfaces **6**, 1158–1163 (2014).

[30]S. Sahoo, A. P. S. Gaur, M. Ahmadi, M. J.-F. Guinel, and R. S. Katiyar, "Temperature-dependent Raman studies and thermal conductivity of few-layer MoS_2," The Journal of Physical Chemistry C **117**, 9042–9047 (2013).
[31]X. Zhang, D. Sun, Y. Li, G.-H. Lee, X. Cui, D. Chenet, Y. You, T. F. Heinz, and J. C. Hone, "Measurement of lateral and interfacial thermal conductivity of single- and bilayer MoS_2 and $MoSe_2$ using refined optothermal Raman technique," ACS Applied Materials & Interfaces **7**, 25923–25929 (2015).
[32]D. J. Late, S. N. Shirodkar, U. V. Waghmare, V. P. Dravid, and C. N. R. Rao, "Thermal expansion, anharmonicity and temperature-dependent Raman spectra of single- and few-layer $MoSe_2$ and WSe_2," ChemPhysChem **15**, 1592–1598 (2014).
[33]N. Peimyoo, J. Shang, W. Yang, Y. Wang, C. Cong, and T. Yu, "Thermal conductivity determination of suspended mono- and bilayer WS_2 by Raman spectroscopy," Nano Research **8**, 1210–1221 (2015).
[34]R. Yan, J. R. Simpson, S. Bertolazzi, J. Brivio, M. Watson, X. Wu, A. Kis, T. Luo, A. R. Hight Walker, and H. G. Xing, "Thermal conductivity of monolayer molybdenum disulfide obtained from temperature-dependent Raman spectroscopy," ACS Nano **8**, 986–993 (2014).
[35]D. J. Late, "Temperature dependent phonon shifts in few-layer black phosphorus," ACS Applied Materials & Interfaces **7**, 5857–5862 (2015).
[36]A. Berkdemir, H. R. Gutiérrez, A. R. Botello-Méndez, N. Perea-López, A. L. Elías, C.-I. Chia, B. Wang, V. H. Crespi, F. López-Urías, J.-C. Charlier, H. Terrones, and M. Terrones, "Identification of individual and few layers of WS_2 using Raman spectroscopy," Scientific Reports **3**, 1755 (2013).
[37]C. Bousige, F. Balima, D. Machon, G. S. Pinheiro, A. Torres-Dias, J. Nicolle, D. Kalita, N. Bendiab, L. Marty, V. Bouchiat, G. Montagnac, A. G. Souza Filho, P. Poncharal, and A. San-Miguel, "Biaxial strain transfer in supported graphene," Nano Letters **17**, 21–27 (2017).
[38]R. S. Alencar, K. D. A. Saboia, D. Machon, G. Montagnac, V. Meunier, O. P. Ferreira, A. San-Miguel, and A. G. Souza Filho, "Atomic-layered MoS_2 on SiO_2 under high pressure: Bimodal adhesion and biaxial strain effects," Phys. Rev. Materials **1**, 024002 (2017).
[39]D. Machon, C. Bousige, R. Alencar, A. Torres-Dias, F. Balima, J. Nicolle, G. de Sousa Pinheiro, A. G. Souza Filho, and A. San-Miguel, "Raman scattering studies of graphene under high pressure," Journal of Raman Spectroscopy **49**, 121–129 (2018), jRS-17-0165.R1.
[40]X.-L. Li, W.-P. Han, J.-B. Wu, X.-F. Qiao, J. Zhang, and P.-H. Tan, "Layer-number dependent optical properties of 2d materials and their application for thickness determination," Advanced Functional Materials **27**, 1604468 (2017).
[41]A. S. Pawbake, M. S. Pawar, S. R. Jadkar, and D. J. Late, "Large area chemical vapor deposition of monolayer transition metal dichalcogenides and their temperature dependent Raman spectroscopy studies," Nanoscale **8**, 3008–3018 (2016).
[42]D. J. Late, U. Maitra, L. S. Panchakarla, U. V. Waghmare, and C. N. R. Rao, "Temperature effects on the Raman spectra of graphenes: Dependence on the number of layers and doping," Journal of Physics: Condensed Matter **23**, 055303 (2011).
[43]X. Luo, Y. Zhao, J. Zhang, M. Toh, C. Kloc, Q. Xiong, and S. Y. Quek, "Effects of lower symmetry and dimensionality on Raman spectra in two-dimensional WSe_2," Phys. Rev. B **88**, 195313 (2013).
[44]H. Li, J. Wu, X. Huang, G. Lu, J. Yang, X. Lu, Q. Xiong, and H. Zhang, "Rapid and reliable thickness identification of two-dimensional nanosheets using optical microscopy," ACS Nano **7**, 10344–10353 (2013).
[45]W. Zhao, Z. Ghorannevis, K. K. Amara, J. R. Pang, M. Toh, X. Zhang, C. Kloc, P. H. Tan, and G. Eda, "Lattice dynamics in mono- and few-layer sheets of WS_2 and WSe_2," Nanoscale **5**, 9677–9683 (2013).
[46]X. Zhang, X.-F. Qiao, W. Shi, J.-B. Wu, D.-S. Jiang, and P.-H. Tan, "Phonon and Raman scattering of two-dimensional transition metal dichalcogenides from monolayer, multilayer to bulk material," Chem. Soc. Rev. **44**, 2757–2785 (2015).
[47]H. Sahin, S. Tongay, S. Horzum, W. Fan, J. Zhou, J. Li, J. Wu, and F. M. Peeters, "Anomalous Raman spectra and thickness-dependent electronic properties of WSe_2," Phys. Rev. B **87**, 165409 (2013).
[48]J. Ribeiro-Soares, R. Almeida, E. B. Barros, P. T. Araujo, M. S. Dresselhaus, L. G. Cançado, and A. Jorio, "Group theory analysis of phonons in two-dimensional transition metal dichalcogenides," Physical Review B **90**, 115438 (2014).
[49]E. del Corro, H. Terrones, A. Elias, C. Fantini, S. Feng, M. A. Nguyen, T. E. Mallouk, M. Terrones, and M. A. Pimenta, "Excited excitonic states in 1l, 2l, 3l, and bulk WSe_2 observed by resonant Raman spectroscopy," ACS Nano **8**, 9629–9635 (2014).
[50]D. J. Late, S. N. Shirodkar, U. V. Waghmare, V. P. Dravid, and C. N. R. Rao, "Thermal expansion, anharmonicity and temperature-dependent Raman spectra of single- and few-layer $MoSe_2$ and WSe_2," ChemPhysChem **15**, 1592–1598 (2014).
[51]M. Yang, X. Cheng, Y. Li, Y. Ren, M. Liu, and Z. Qi, "Anharmonicity of monolayer MoS_2, $MoSe_2$, and WSe_2: A Raman study under high pressure and elevated temperature," Applied Physics Letters **110**, 093108 (2017).
[52]S. V. Bhatt, M. P. Deshpande, V. Sathe, R. Rao, and S. H. Chaki, "Raman spectroscopic investigations on transition-metal dichalcogenides MX_2 (M = Mo, W; X = S, Se) at high pressures and low temperature," Journal of Raman Spectroscopy **45**, 971–979 (2014).
[53]M. Balkanski, R. F. Wallis, and E. Haro, "Anharmonic effects in light scattering due to optical phonons in silicon," Phys. Rev. B **28**, 1928–1934 (1983).
[54]P. S. Peercy and B. Morosin, "Pressure and temperature dependences of the Raman-active phonons in SnO_2," Phys. Rev. B **7**, 2779–2786 (1973).
[55]G. Slack, "Nonmetallic crystals with high thermal conductivity," Journal of Physics and Chemistry of Solids **34**, 321–335 (1973).
[56]M. Steiner, M. Freitag, V. Perebeinos, J. C. Tsang, J. P. Small, M. Kinoshita, D. Yuan, J. Liu, and P. Avouris, "Phonon populations and electrical power dissipation in carbon nanotube transistors," Nature Nanotechnology **4**, 320–324 (2009).
[57]S. Berciaud, M. Y. Han, K. F. Mak, L. E. Brus, P. Kim, and T. F. Heinz, "Electron and optical phonon temperatures in electrically biased graphene," Phys. Rev. Lett. **104**, 227401 (2010).
[58]Z. Tian, K. Esfarjani, J. Shiomi, A. S. Henry, and G. Chen, "On the importance of optical phonons to thermal conductivity in nanostructures," Applied Physics Letters **99**, 053122 (2011).
[59]R. S. Alencar, C. Rabelo, H. L. S. Miranda, T. L. Vasconcelos, B. S. Oliveira, A. Ribeiro, J. Ribeiro-Soares, A. G. S. Filho, L. G. Cançado, and A. Jorio, "Probing spatial phonon correlation length in post-transition metal monochalcogenide gas using tip-enhanced Raman spectroscopy" (submitted).